suppressed in TSLP receptor-deficient mice [7]. In addition, the intratrachial administration of Fc-TSLP receptor-fusion protein or anti-TSLP receptor significantly reduced eosinophil infiltration, hyperplasia, and Th2 cytokine production [7, 8]. Lung-specific expression of TSLP induced asthma-like airway inflammation [9], and skin-selective expression and intradermal injection of TSLP induced atopic dermatitis [10, 11]. Thus, an excess of TSLP is enough to cause allergic inflammation.

TSLP induces the activation of immature dendritic cells, recruitment of mature dendritic cells into lymph nodes, and expression of the OX40 ligand (OX40L) [12], which triggers the differentiation of allergen-specific naïve CD4+ T cells into inflammatory Th2 cells that produce IL-4, IL-5, IL-13 and TNF-α [12, 13].

It has been reported that epithelial cells (e.g. airway epithelial cells and keratinocytes) and mast cells produce TSLP when stimulated with antigens, cytokines and Toll-like receptor ligands [2, 14–16]. The production of TSLP by epithelial cells was significantly enhanced by TNF-α and/or IL-4 [14, 15]. Authors have reported that the application of 12-O-tetradecanoylphorbol-13-acetate (TPA) to the earlobes of mice induced the expression of TSLP mRNA [17]. The findings indicated that the production of TSLP could be induced by nonimmunological stimulants such as chemical compounds.

The first cells to interact with chemical compounds in the environment are the epithelial cells of the respiratory system, digestive tract and skin. Therefore, chemicals that promote Th2-type reactions and worsen allergic inflammation might induce TSLP production by epithelial cells. To clarify the involvement of TSLP in the induction of Th2-type reactions, we used our novel allergic inflammation model using picryl chloride (PiCl), a contact-sensitizing chemical [17]. PiCl induced Th1-dominant contact hypersensitivity in the mice treated with cyclophosphamide, which causes blood eosinophils [18] and decreases the number of regulatory T cells [19]. However, the application of TPA after the sensitization with PiCl, which induces TSLP production, shifted the PiCl-induced allergic inflammation from a delayed-type response to a biphasic response, increased the infiltration of eosinophils, and the cytokine milieu from Th1 to Th2 [17]. Thus, this model is useful for detecting the chemical such as TPA, which shifts the cytokine milieu from Th1 to Th2 by producing TSLP.

In this study, the activity of various organic solvents to elicit TSLP production was examined in vivo and xylene was found to potentially augment Th2-type allergic responses by inducing TSLP production.

Animals and Methods

Animals

Male BALB/c mice and C57BL/6 (5 weeks old), WBBF1 wild-type, and W/W^v mice were purchased from SLC (Shizuoka, Japan). The generation of TSLP receptor knockout mice (C57BL/6 background) has been described previously [20]. BALB/c TNF-α knockout mice (BALB/c background) were established from original TNF-α knockout mice [21]. IL-4 receptor α-chain gene knockout mice (BALB/c background) [22, 23] were purchased from Immuno-Biological Laboratories, Co. Ltd. (Takasaki, Japan). The study protocol was approved by the Institutional Animal Care and Use Committee of Tohoku University (Permission No. 20-Pharma-Animal-22).

Assay of TSLP Production Triggered by Organic Solvents

The organic solvents used were benzene, chloroform, ethyl acetate, toluene, xylene, xylene isomers, 1,3,5-trimethylbenzene, and 1,2,4-trimethylbenzene (Wako Pure Chemical Industries, Osaka, Japan) and TPA (Sigma-Aldrich, St. Louis, Mo., USA). Twenty microliters of solvent or a 0.04-μg/μl TPA solution (3:1 in acetone:ethanol) was painted on the right earlobe of mice. Earlobe tissue was then punched out (diameter 5 mm) at a specified time and weighed.

Determination of the Expression of mRNA for TSLP in Earlobes

The total RNA of tissues was extracted using a GenElute Mammalian Total RNA Kit (Sigma-Aldrich) according to the manufacturer's instructions. The extracted RNA (0.5 μg) was reverse-transcribed by using M-MLV reverse transcriptase (Invitrogen Co., Carlsbad, Calif., USA). PCR amplification of the cDNA was performed with *Taq* polymerase (Takara, Ohtsu, Japan) and specific primers. The sequences of the primers used and PCR conditions for the amplification of TSLP cDNA were: (forward) 5′-GAC AGC ATG GTT CTT CTC AG-3′ and (reverse) 5′-CTG GAG ATT GCA TGA AGG-3′, 40 cycles of denaturation at 94°C for 1 min, annealing at 57°C for 1 min, and extension at 72°C for 1 min. The murine glyceraldehyde 3-phosphate dehydrogenase (GAPDH) gene (a housekeeping gene) was used as an internal standard. The sequences of primers used for the amplification of GAPDH cDNA were: (forward) 5′-TGA TGA CAT CAA GAA GGT GGT GAA G-3′ and (reverse) 5′-TCC TTG GAG GCC ATG TAG GCC AT-3′. PCR was performed for 27 cycles, denaturation at 94°C for 0.5 min, annealing at 57°C for 1 min, and extension at 72°C for 2 min.

Determination of TSLP Protein in the Tissue

The tissue samples were homogenated at 4°C in 10 vol of phosphate-buffered saline by a Beads Cell Disrupter (MS-100, Tomy Digital Biology Co., Tokyo, Japan). The concentration of TSLP in the supernatant of the homogenate was determined by ELISA (R&D Systems, Minneapolis, Minn., USA). The supernatant contains unidentified substances which nonspecifically bind to the biotin-labeled enzyme of the ELISA kit. Therefore, the level of TSLP in the supernatant was measured with or without a secondary antibody to recognize nonspecific binding. The value obtained with the homogenate of untreated earlobes was then subtracted from the data to give the increase in the level of TSLP.

Histological Analysis

The earlobe tissue was excised 24 h after the painting of xylene and immediately fixed in 10% neutral buffered formalin and embedded in paraffin. The sections were immunostained or stained with hematoxylin and eosin. The immunostaining of TSLP was performed using a rabbit anti-human TSLP antibody (Santa Cruz Biotechnology Inc., Santa Cruz, Calif., USA) and the avidin-biotin-peroxidase system (Vector Laboratories Inc., Burlingame, Calif., USA).

Determination of OX40L mRNA Levels in Cervical Lymph Nodes

Xylene (20 μl) was painted on the right ear of mice once or once a day for 7 days. Twenty-four hours after the last painting, the cervical lymph nodes were excised and weighed. cDNA was prepared as described above. The sequences of the primers used and conditions for the amplification of OX40L cDNA were as follows: (forward) 5′-CAG AGG AGC AGT TAC CAG AT-3′ and (reverse) 5′-CAG GAG CAT TTA CAG TCA GG-3′, 31 cycles of denaturation at 94°C for 1 min, annealing at 58°C for 1 min, and extension at 72°C for 1 min. The levels of mRNA for OX40L and GAPDH were quantitated by scanning densitometry, and the density ratio of the OX40L mRNA to the GAPDH mRNA was calculated.

Induction of PiCl-Induced Allergic Inflammation and Determination of IL-4

The effects of xylene on PiCl-induced contact dermatitis were examined as reported [17]. Briefly, cyclophosphamide (Sigma-Aldrich) was dissolved in saline and injected subcutaneously at a dose of 150 mg/kg into TSLP receptor knockout mice and wild-type mice. Two days later, mice were sensitized with 50 μl of a 7% (w/v) PiCl solution (Nacalai Tesque, Kyoto, Japan; 3:1 in acetone:ethanol; day 0). Thereafter, 20 μl of xylene was applied to the same site twice (days 5 and 10). On day 12, mice were challenged with 20 μl of a 1% (w/v) PiCl solution by painting it on the right earlobe. Ear thickness was measured with a dial thickness gauge (Peacock, Ozaki, Tokyo, Japan) at a specified time. A homogenate of earlobe tissues was prepared as described above and the level of IL-4 was determined by ELISA (e-Biosciences Inc., San Diego, Calif., USA). Nonspecific binding was subtracted as described above.

Statistical Significance

The statistical significance of the results was analyzed with the Dunnett test or the Student-Newman-Keuls test for multiple comparisons. The results were confirmed by at least three independent sets of experiments.

Results

TSLP Production Induced by Organic Solvents

Various organic solvents were painted on the right earlobes of mice. Consistent with previous findings [17], TPA induced the expression of TSLP mRNA in the earlobes excised 4 h after the painting (fig. 1). Under these conditions, the application of toluene and xylene, but not chloroform or ethyl acetate, induced the expression of TSLP mRNA (fig. 1). The effects of aromatic compounds on the production of TSLP protein were then examined. TPA also induced the increase in TSLP protein in the homogenate of earlobe tissue excised 24 h after the painting, and the amount of TSLP (increase vs. untreated) was 515 ± 18 pg/ml. Xylene but not benzene increased the level of TSLP in the homogenate (table 1). The level of activity of toluene was in between that of xylene and benzene. Because the xylene used was a mixture of 3 isomers, *o*-xylene, *m*-xylene and *p*-xylene (1:5:3), the activity of each isomer was determined. Interestingly, *m*-xylene induced

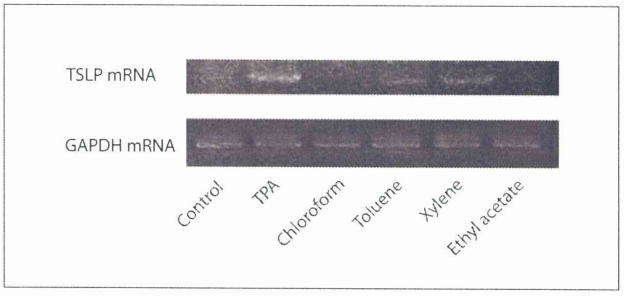

Fig. 1. Effects of chemical compounds on the expression of TSLP mRNA. Twenty microliters each of a 0.04 μg/μl TPA solution, chloroform, toluene, xylene and ethyl acetate were painted on the earlobes of BALB/c mice. Four hours later, total RNA was extracted from the excised earlobe tissue and the mRNAs for TSLP and GAPDH were detected by RT-PCR.

Table 1. Induction of TSLP by organic solvents

Organic solvent	TSLP (increase vs. untreated), pg/ml
No solvent	0 ± 74
Benzene	53 ± 96
Toluene	249 ± 68*
Xylene	579 ± 128**
o-Xylene	154 ± 68
m-Xylene	801 ± 145**
p-Xylene	345 ± 90**
1,2,4-Trimethylbenzene	2,178 ± 279**
1,3,5-Trimethylbenzene	1,531 ± 184**

Organic solvents (20 μl) were painted on the right earlobe of BALB/c mice. The earlobe tissue was excised 24 h after the painting and the level of TSLP in the tissue homogenate was determined by ELISA. Data are shown as the mean ± SEM for 6–10 mice. Statistical significance: * $p < 0.05$ and ** $p < 0.01$ vs. with no solvent.

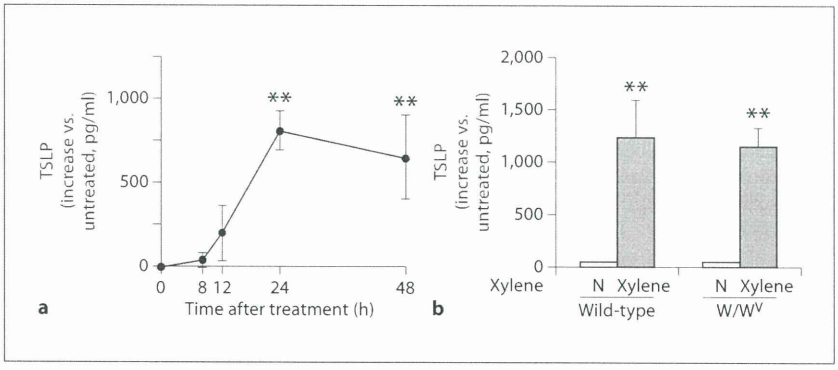

Fig. 2. Induction by xylene of TSLP production in earlobe tissue. **a** Xylene (20 μl) was painted on the right earlobe of BALB/c mice. TSLP levels were determined at the indicated time points after the treatment. Data are shown as the mean ± SEM for 4–5 mice, ** $p < 0.01$ versus time 0. **b** Xylene was painted on the earlobes of WBBF1 W/W^v mice and the corresponding wild-type mice (grey columns). The earlobes were excised 24 h after the treatment. N = Non-treated group. Data are shown as the mean ± SEM for 5 mice, ** $p < 0.01$ versus the corresponding N.

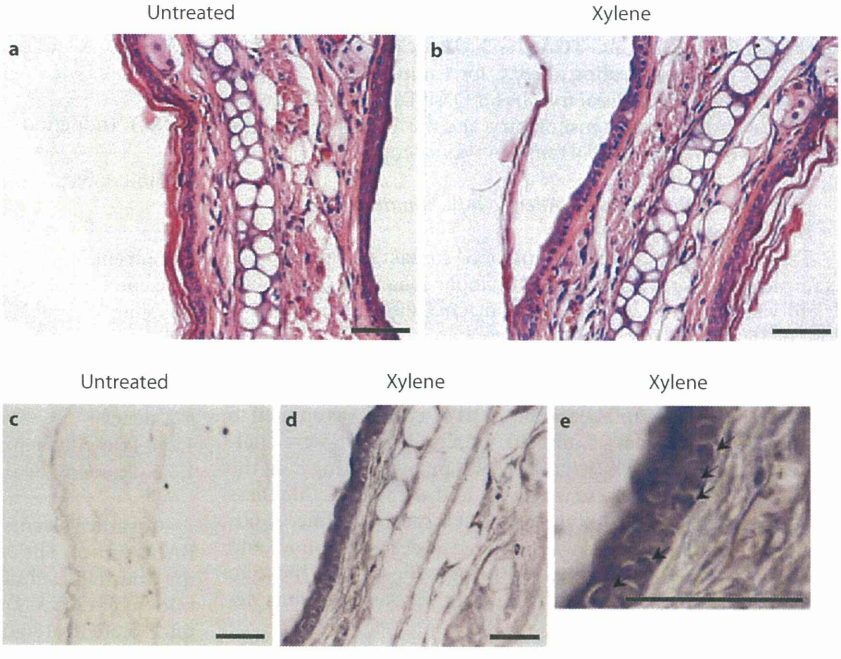

Fig. 3. Histochemical analysis of TSLP-producing cells. Xylene was painted on the right earlobe of BALB/c mice. The tissue of right earlobe tissue (**b**, **d**, **e**) and the left earlobe (untreated ear, **a**, **c**) were excised 24 h after the treatment. Tissue sections were stained with hematoxylin and eosin (**a**, **b**) and anti-TSLP antibody (**c**–**e**). **e** This is a higher magnification of **d**. The positive cells were indicated with arrows. The scale bar represents 100 (**a**, **b**) and 50 μm (**c**–**e**).

the production of TSLP much more extensively than did *o*-xylene (table 1). Furthermore, both 1,3,5-trimethylbenzene and 1,2,4-trimethylbenzene also triggered marked TSLP production (table 1). Since the xylene identified in indoor environments is a mixture of 3 isomers, we used xylene as a chemical inducer of TSLP production in subsequent experiments.

TSLP-Producing Cells

The level of TSLP in the xylene-treated earlobes slowly increased and reached a maximum at 24 h (fig. 2a). The painting of xylene on the earlobes of mast cell-deficient W/W^v mice caused the production of TSLP at 24 h to almost the same extent as in the corresponding control mice (fig. 2b). The painting of xylene almost did not induce the infiltration of leukocytes (fig. 3a, b). The immunostaining with anti-TSLP disclosed that the TSLP-producing cells were mainly located in the epithelial layer of the xylene-treated ear (fig. 3d, e).

Involvement of TNF-α and IL-4 in the Xylene-Induced Production of TSLP

To clarify whether TNF-α and IL-4 enhanced xylene-induced production of TSLP, xylene was painted on the

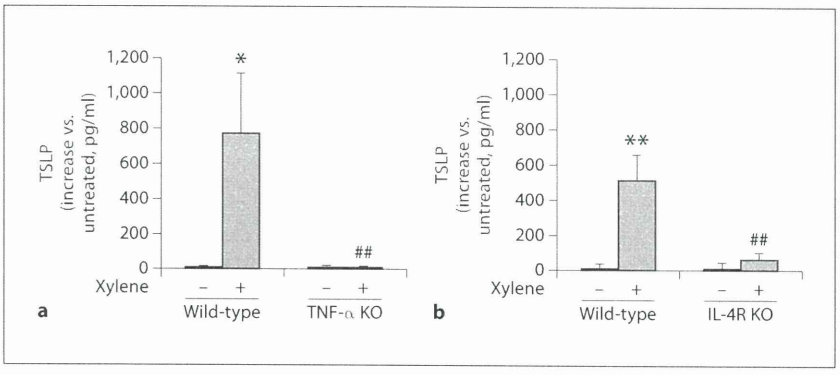

Fig. 4. Xylene-induced production of TSLP in earlobes of TNF-α knockout mice and IL-4 receptor knockout mice. Xylene (20 μl) was painted on the right earlobe of BALB/c wild-type mice and TNF-α knockout mice (TNF-α KO; **a**) and IL-4 receptor knockout mice (IL-4R KO; **b**). The earlobes were excised 24 h later. The concentration of TSLP in the supernatant of the earlobe homogenate was determined by ELISA. Data are shown as the mean ± SEM for 7 mice, * $p < 0.05$, ** $p < 0.01$ versus without xylene (–), ## $p < 0.01$ versus with xylene (+) in wild-type mice.

earlobes of TNF-α knockout mice and IL-4 receptor knockout mice. In these knockout mice, xylene-induced TSLP production was significantly diminished (fig. 4).

Increase in the Weight of Cervical Lymph Nodes and Expression of OX40L on the Painting of Xylene

To clarify whether or not xylene caused the production of a significant amount of TSLP to activate dendritic cells, the weight of the cervical lymph node and the expression of OX40L were determined. Although not significantly increased 1 day after the painting of xylene, the weight of the cervical lymph node was significantly greater following repeated treatment with xylene for 7 days (fig. 5a). The xylene-induced increase was smaller in C57BL/6 mice (fig. 5b) than in BALB/c mice, and partially but significantly reduced in TSLP receptor knockout mice (fig. 5b). In addition, the level of OX40L mRNA in the lymph node was apparently increased by the repeated treatment with xylene in wild-type mice but not in TSLP receptor knockout mice (fig. 5c, d).

Exacerbation of PiCl-Induced Allergic Inflammation by Xylene

Finally, the possibility was examined that xylene exacerbated antigen-induced allergic inflammation via TSLP production. As shown in figure 6a, the painting of xylene on the same earlobes 5 and 10 days after the sensitization with PiCl enhanced the PiCl-induced increase in ear thickness. The levels of IL-4 in the earlobe tissue 24 h after the challenge were also increased by the application of xylene (fig. 6b). The enhancement by xylene of ear swelling and IL-4 production was not observed in TSLP receptor knockout mice (fig. 6).

Discussion

TSLP is a master cytokine inducing Th2-type allergic inflammation [3]. In our study, some organic chemicals, i.e. volatile solvents used in paints and glues, induced production of TSLP, resulting in an exacerbation of allergic inflammation.

Among the organic solvents tested, xylene, especially *m*-xylene, 1,3,5-trimethylbenzene and 1,2,4-trimethylbenzene significantly caused the production of TSLP in vivo (fig. 1, table 1). Interestingly, the activity to induce TSLP production was highly dependent on the position of methyl groups on the benzene ring. Namely, *m*-xylene induced much more extensively the production of TSLP than did *o*-xylene. These findings suggested that xylene triggered TSLP production by binding to a specific protein in a structure-dependent manner, and not via physical and/or chemical toxicity.

The TSLP-producing cells were mainly epithelial cells and mast cells [1, 2]. In addition, mast cells induced epithelial TSLP production in a model of allergic rhinitis [24]. However, the painting of xylene on the earlobes of mast cell-deficient W/W^v mice caused the production of TSLP to almost the same extent as in the corresponding control mice (fig. 2b), indicating that mast cells were not involved in the xylene-induced production of TSLP. The painting of xylene almost did not induce the infiltration of leukocytes, indicating that the cells existing in the skin might be producing TSLP. The immunostaining analysis disclosed that the TSLP-producing cells were mainly located in the epithelial layer of the xylene-treated ear (fig. 3d, e). These findings suggested that the cells, such as keratinocytes, in the epithelial layer produced TSLP in response to xylene.

TNF-α and IL-4 only slightly induced production of TSLP but enhanced Toll-like receptor ligand-induced

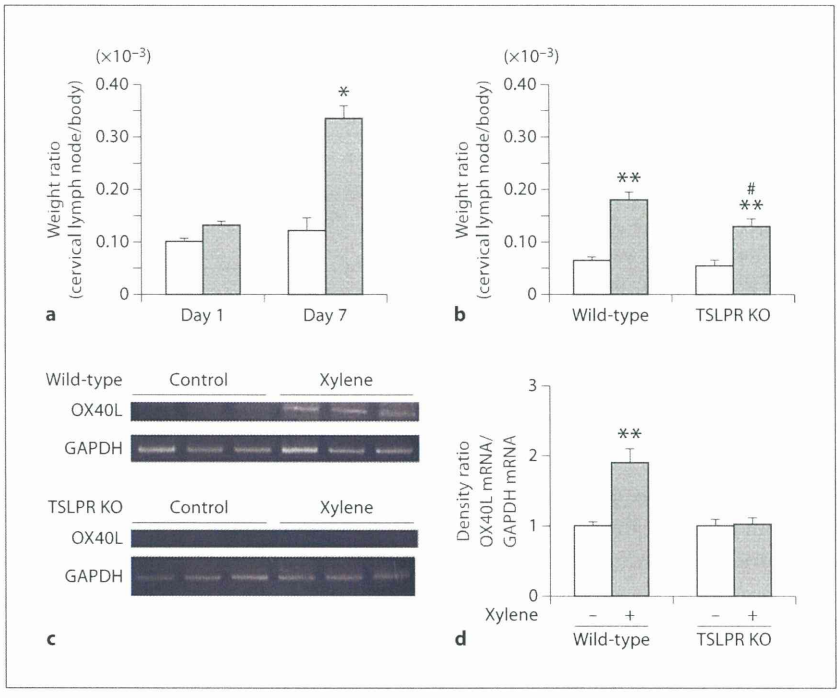

Fig. 5. Xylene-induced increase in the weight of the cervical lymph node and expression of OX40L. **a**, **b** Xylene was painted on the earlobe of BALB/c mice once or once a day for 7 days (**a**) or of TSLP receptor knockout mice and the corresponding wild-type mice (C57BL/6) once a day for 7 days (**b**). The cervical lymph nodes were excised 24 h after the last treatment. The weight of the cervical lymph node relative to body weight was determined. Grey columns indicate the xylene-treated group and open columns indicate the untreated group. Data are shown as the mean ± SEM for 5 mice, * $p < 0.05$, ** $p < 0.01$ versus the corresponding untreated group, # $p < 0.05$ versus the corresponding wild-type mice. **c**, **d** The expression of OX40L mRNA in the lymph nodes excised from wild-type mice and TSLP receptor knockout mice treated with xylene for 7 days was determined by RT-PCR. Data indicate the results for 3 mice in each group. The density ratio of OX40L mRNA to GAPDH mRNA was calculated (**d**). The mean density ratio of the untreated group was set to 1.0. Data are shown as the mean ± SEM for 3 mice, ** $p < 0.01$ versus the corresponding untreated group.

production in vitro [14–16]. No increase in the levels of these cytokines in the earlobe tissue obtained 4–24 h after the painting of xylene was detected (data not shown). However, xylene-induced production of TSLP was significantly diminished in TNF-α knockout mice and IL-4 receptor knockout mice (fig. 4), indicating that xylene elicited TSLP production via costimulation with basal or low levels of TNF-α and IL-4. The producing cells of TNF-α and IL-4 might be the responding cells to xylene, but they were not identified via the immunostaining (data not shown). These findings also suggested that there is a common pathway triggered by xylene and Toll-like receptor ligands. The molecular mechanisms by which xylene induces TSLP production are under investigation.

TSLP induces the expression of OX40L on dendritic cells [12] and the proliferation of Th2 lymphocytes [12, 13]. In the previous model, xylene increased the weight of the cervical lymph node and the expression of OX40L (fig. 5). Because these responses were reduced in TSLP receptor knockout mice, it was likely that xylene triggered the activation of dendritic cells via the production of TSLP, resulting in an increase in the proliferation of lymphocytes in the cervical lymph nodes. Because the weight of the lymph node was increased by xylene in TSLP receptor knockout mice, the possibility that xylene induced the production of cytokines other than TSLP, which caused lymphocytes to proliferate, could not be ruled out.

Some chemical compounds, such as formalin, bind to proteins and act as a hapten to induce allergies. The antigenicity of xylene itself, however, has not been reported. It is possible that xylene exacerbated the antigen-induced

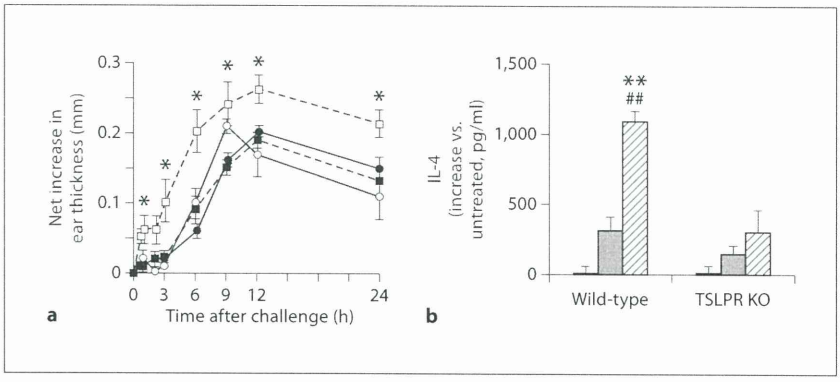

Fig. 6. Exacerbation of PiCl-induced allergic inflammation by xylene. **a** C57BL/6 wild-type mice (squares) and TSLP receptor knockout mice (circles) were pretreated with cyclophosphamide (150 mg/kg) on day –2 and 50 μl of a 7% (w/v) PiCl solution was painted on the right earlobe on day 0. The sensitized mice were treated with xylene at the same site on days 5 and 10 (open symbols) or left untreated (closed symbols). On day 12, mice were challenged with 20 μl of a 1% (w/v) PiCl solution painted on the right earlobe. Earlobe thickness was measured 0–24 h after the challenge. Ear thickness before the challenge was subtracted from the data. Data are shown as the mean ± SEM for 5 mice, * $p < 0.05$ versus the corresponding PiCl-treated group. **b** The concentration of IL-4 in homogenate of the earlobe tissue excised 24 h after the PiCl challenge was determined by ELISA. Open columns, hatched columns and grey columns indicate the untreated group, PiCl-treated group and PiCl + xylene-treated group, respectively. Data are shown as the mean ± SEM for 5 mice, ** $p < 0.01$ versus the corresponding untreated group, ## $p < 0.01$ versus the corresponding PiCl-treated group.

allergic inflammation via TSLP production. Authors have reported that the application of TPA aggravated PiCl-induced allergic inflammation [17]. In that model, TPA elicited the production of TSLP and shifted the cytokine milieu from Th1 to Th2 [17]. In our study, xylene, which was used instead of TPA, enhanced the PiCl-induced thickening of the ear and IL-4 production (fig. 6). Xylene failed to induce a biphasic response which was observed by PiCl plus TPA [17]. The discrepancy might be caused by the use of a different mouse strain. In the previous study, we used Balb/c mice, i.e. Th2-oriented mice, but in this study, we used C57BL/6 mice, i.e. Th1-oriented mice, because the TSLP receptor knockout mice we used had a C57BL/6 background. The finding that the xylene-induced enhancement of these responses was reversed in TSLP receptor knockout mice suggested that xylene exacerbated the PiCl-induced allergic inflammation via production of TSLP, which elicited an enhancement of Th2-type immune responses as determined from IL-4 levels.

Xylene, 1,3,5-trimethylbenzene and 1,2,4-trimethylbenzene are volatile solvents of paints and glues and often detected in indoor environments [25]. Recently, it was reported that repeated exposure to a cigarette smoke extract induced TSLP production and promoted antigen-induced Th2-type immune responses and airway inflammation [26]. Therefore, the inhalation of these organic solvents may also induce TSLP production in respiratory tissue and exacerbate asthma and allergic rhinitis. Authors have now begun studying this possibility.

In conclusion, xylene induced the production of TSLP and aggravated allergic inflammation. This is the first report of a pure chemical compound detected in the environment triggering TSLP production and worsening allergic inflammation in vivo. The models employed here would be useful for detecting chemicals that exacerbate allergic inflammation without antigenicity. In addition, xylene might be a good tool for examining the role of TSLP in eliciting allergy in experimental animals.

Acknowledgements

This study was supported in part through a grant of the Long Range Research Initiative (LRI) by the Japan Chemical Industry Association (JCIA), Grant-in-Aid for Challenging Exploratory Research (22659025) from the Japan Society for the Promotion of Science, and by the Division of Intramural Research, National Heart, Lung, and Blood Institute, NIH.

References

1 Sims JE, Williams DE, Morrissey PJ, Garka K, Foxworthe D, Price V, Friend SL, Farr A, Bedell MA, Jenkins NA, Copeland NG, Grabstein K, Paxton RJ: Molecular cloning and biological characterization of a novel murine lymphoid growth factor. J Exp Med 2000;192:671–680.

2 Okayama Y, Okumura S, Sagara H, Yuki K, Sasaki T, Watanabe N, Fueki M, Sugiyama K, Takeda K, Fukuda T, Saito H, Ra C: FcepsilonRI-mediated thymic stromal lymphopoietin production by IL-4-primed human mast cells. Eur Respir J 2009;34:425–435.

3 Liu YJ: Thymic stromal lymphopoietin: master switch for allergic inflammation. J Exp Med 2006;203:269–273.

4 Ying S, O'Connor B, Ratoff J, Meng Q, Mallett K, Cousins D, Robinson D, Zhang G, Zhao J, Lee T, Corrigan C: Thymic stromal lymphopoietin expression is increased in asthmatic airways and correlates with expression of Th2-attracting chemokines and disease severity. J Immunol 2005;174:8183–8190.

5 Soumelis V, Reche P, Kanzler H, Yuan W, Edward G, Homey B, Gilliet M, Ho S, Antonenko S, Lauerma A, Smith K, Gorman D, Zurawski S, Abrams J, Menon S, McClanahan T, de Waal-Malefyt Rd R, Bazan F, Kastelein R, Liu Y: Human epithelial cells trigger dendritic cell mediated allergic inflammation by producing TSLP. Nat Immunol 2002;3:673–680.

6 Miyata M, Hatsushika K, Ando T, Shimokawa N, Ohnuma Y, Katoh R, Suto H, Ogawa H, Masuyama K, Nakao A: Mast cell regulation of epithelial TSLP expression plays an important role in the development of allergic rhinitis. Eur J Immunol 2008;38:1487–1492.

7 Al-Shami A, Spolski R, Kelly J, Keane-Myers A, Leonard W: A role for TSLP in the development of inflammation in an asthma model. J Exp Med 2005;202:829–839.

8 Shi L, Leu SW, Xu F, Zhou X, Yin H, Cai L, Zhang L: Local blockade of TSLP receptor alleviated allergic disease by regulating airway dendritic cells. Clin Immunol 2008;129:202–210.

9 Zhang K, Shan L, Rahman MS, Unruz H, Halayko AJ, Gounni AS: Constitutive and inducible thymic stromal lymphopoietin expression in human airway smooth muscle cells: role in chronic obstructive pulmonary disease. Am J Physiol Lung Cell Mol Physiol 2007;293:L375–L382.

10 Yoo J, Omori M, Gyarmati D, Zhou B, Aye T, Brewer A, Comeau M, Campbell D, Ziegler S: Spontaneous atopic dermatitis in mice expressing an inducible thymic stromal lymphopoietin transgene specifically in the skin. J Exp Med 2005;202:541–549.

11 Jessup H, Brewer A, Omori M, Rickel E, Budelsky A, Yoon B, Ziegler S, Comeau M: Intradermal administration of thymic stromal lymphopoietin induces a T cell- and eosinophil-dependent systemic Th2 inflammatory response. J Immunol 2008;181:4311–4319.

12 Ito T, Wang YH, Duramad O, Hori T, Delespesse GJ, Watanabe N, Qin FX, Yao Z, Cao W, Liu YJ: TSLP-activated dendritic cells induce an inflammatory T helper type 2 cell response through OX40 ligand. J Exp Med 2005;202:1213–1223.

13 Liu YJ: Thymic stromal lymphopoietin and OX40 ligand pathway in the initiation of dendritic cell-mediated allergic inflammation. J Allergy Clin Immunol 2007;120:238–244.

14 Kato A, Favoreto Jr S, Avila PC, Schleimer RP: TLR3- and Th2 cytokine-dependent production of thymic stromal lymphopoietin in human airway epithelial cells. J Immunol 2007;179:1080–1087.

15 Bogiatzi SI, Fernandez I, Bichet JC, Marloie-Provost MA, Volpe E, Sastre X, Soumelis V: Proinflammatory and Th2 cytokines synergize to induce thymic stromal lymphopoietin production by human skin keratinocytes. J Immunol 2007;178:3373–3377.

16 Allakhverdi Z, Comeau MR, Jessup HK, Yoon BR, Brewer A, Chartier S, Paquette N, Ziegler SF, Sarfati M, Delespesse G: Thymic stromal lymphopietin is released by human epithelial cells in response to microbes, trauma, or inflammation and potently activates mast cells. J Exp Med 2007;204:253–258.

17 Hirasawa N, Ohsawa Y, Katoh G, Shibata K, Ishihara K, Seyama T, Tamura S, Hong JJ, Ohuchi K: Modification of the picryl chloride-induced allergic dermatitis model in mouse earlobes by 12-O-tetradecanoylphorbol 13-acetate, and analysis of the role of histamine in the modified model. Int Arch Allergy Immun 2009;148:279–288.

18 Satoh T, Cheu QJ, Sasaki G, Yokozeki H, Katayama I, Nishioka K: Cyclophosphamide-induced blood and tissue eosinophilia in contact sensitivity: mechanism of hapten-induced eosinophil recruitment into the skin. Eur J Immunol 1997;27:85–91.

19 Ikezawa Y, Nakazawa M, Tamura C, Takahashi K, Minami M, Ikezawa Z: Cyclophosphamide decreases the number, percentage and the function of CD25+ CD4+ regulatory T cells, which suppress induction of contact hypersensitivity. J Dermatol Sci 2005;39:105–112.

20 Al-Shami A, Spolski R, Kelly J, Fry T, Schwartzberg P, Pandey A, Mackall C, Leonard W: A role for thymic stromal lymphopoietin in CD4(+) T cell development. J Exp Med 2004;200:159–168.

21 Tagawa Y, Sekikawa K, Iwakura Y: Suppression of concanavalin A-induced hepatitis in IFN-γ mice, but not in TNF-α mice. J Immunol 1997;159:1418–1428.

22 Noben-Trauth N, Shultz LD, Brombacher F, Urban JF Jr, Gu H, Paul WE: An interleukin 4 (IL-4)-independent pathway for CD4+ T cell IL-4 production is revealed in IL-4 receptor-deficient mice. Proc Natl Acad Sci USA 1997;94:10838–10843.

23 Noben-Trauth N, Paul WE, Sacks DL: IL-4- and IL-4 receptor-deficient BALB/c mice reveal differences in susceptibility to Leishmania major parasite substrains. J Immunol 1999;162:6132–6140.

24 Miyata M, Hatsushika K, Ando T, Shimokawa N, Ohnuma Y, Katoh R, Suto H, Ogawa H, Masuyama K, Nakao A: Mast cell regulation of epithelial TSLP expression plays an important role in the development of allergic rhinitis. Eur J Immunol 2008;38:1487–1492.

25 Azuma K, Uchiyama I, Ikeda K: The risk screening for indoor air pollution chemicals in Japan. Risk Anal 2007;27:1623–1638.

26 Nakamura Y, Miyata M, Ohba T, Ando T, Hatsushika K, Suenaga F, Shimokawa N, Ohnuma Y, Katoh R, Ogawa H, Nakao A: Cigarette smoke extract induces thymic stromal lymphopoietin expression, leading to Th2-type immune responses and airway inflammation. J Allergy Clin Immunol 2008;122:1208–1214.

Journal of Dermatological Science 62 (2011) 50–57

Contents lists available at ScienceDirect

Journal of Dermatological Science

journal homepage: www.elsevier.com/jds

Enhancement of nickel elution by lipopolysaccharide-induced inflammation

Rina Tanaka [a], Yoshiaki Goi [a], Kenji Ishihara [b], Kyosuke Ueda [c], Takayuki Narushima [c], Hiroshi Ohtsu [c], Masahiro Hiratsuka [a], Noriyasu Hirasawa [a,*]

[a] Graduate School of Pharmaceutical Sciences, Tohoku University, Japan
[b] Course for School Nurse Teacher, Faculty of Education, Ibaraki University, Japan
[c] Graduate School of Engineering, Tohoku University, Japan

ARTICLE INFO

Article history:
Received 20 August 2010
Received in revised form 25 December 2010
Accepted 27 December 2010

Keywords:
Nickel release
Lipopolysaccharide
In vivo model
In vitro model
RAW 264 cells

ABSTRACT

Background: Implantations of metallic biomedical devices into bodies are increasing. The elution of Ni ions from these devices can lead to metal allergies. However, the molecular mechanisms of the elution have not been fully examined. Furthermore, it is not clear whether infection and inflammation affect the corrosion of metals.
Objective: We examined whether the elution of Ni from metal wires and plates was enhanced by inflammation *in vivo* and *in vitro*.
Methods: A Ni or SUS316L wire was implanted subcutaneously in the dorsum of mice. Lipopolysaccharide (LPS) was injected at the site immediately following the implantation. After 8, 24, and 72 h, the tissue around the wire was excised. RAW 264 cells were seeded on a Ni plate and incubated for 24 h in medium containing LPS. The amount of Ni in the tissue or conditioned medium was determined fluorometrically.
Results: The release of Ni ions from the wire was significantly increased from 8 to 72 h, and further increased by LPS. LPS also enhanced the release of Ni ions by the cells, but only when they were attached to the Ni plate. Chloroquine, bafilomycin A_1 and amiloride markedly inhibited the effects of LPS.
Conclusion: The activation of inflammatory cells on metals enhanced the elution of Ni probably via the release of protons at the interface of the cells and material.

1. Introduction

Implantations of biomedical devices to treat diseases and organ insufficiencies are increasing as populations age [1]. Most devices for the replacement of hard tissues, including artificial hip joints, bone plates and dental implants, comprise metallic biomaterials because of their reliable mechanical performance [2,3]. Corrosion-resistant and ductile, nickel (Ni) is contained in various alloys, including stainless steels, Ni–Cr and Ni–Ti. However, Ni is also the most common contact allergen among metals [4]. Allergies to Ni, classified as Type IV allergies [5], are initiated by the release of Ni ions from alloys. Ni bound to soluble proteins [4] or to proteins on antigen-presenting cells [6] is recognized as an antigen. The antigen-presenting cells then activate T cells and induce an increase in the number of Ni-specific, IFN-γ-producing $CD4^+$ and $CD8^+$ effector T cells [7]. It is difficult to prevent Ni allergies by inhibiting these immune responses. A more practical approach might be to block the elution of Ni ions from biomaterials. However, the molecular mechanisms of this elution have not been fully examined. Furthermore, although the inflamed sites become acidic, it is not clear whether infection and inflammation affect the corrosion of metals.

In general, the release of Ni ions from alloys is tested in solutions [8,9]. However, as biodevices are implanted for long periods of time, one should test the release of metal ions from alloys in tissues to assess the risk of inducing metal allergies. There is little evidence that the release of metal ions from alloys *in vivo* is similar to that *in vitro*.

To reveal the mechanisms of Ni-induced inflammation and allergy, several animal models have been developed. The injection of Ni ions into sensitized animals was found to cause allergic inflammation including ear swelling [8–10], footpad edema [11] and the proliferation of lymph node cells [12]. Tolerance to nickel sensitization was also examined in these animals [9]. Recently, Sato et al. found that the co-administration of lipopolysaccharide (LPS), a stimulator of innate immune responses [13], effectively enhanced sensitization to Ni [10]. Sensitization using Ni ions plus LPS will promote research into how metal allergies are evoked. In contrast to models using Ni ions, we induced inflammation in mice using a Ni

* Corresponding author at: Laboratory of Pharmacotherapy of Life-style Related Diseases, Graduate School of Pharmaceutical Sciences, Tohoku University, 6-3 Aoba Aramaki, Aoba-ku, Sendai, Miyagi 980-8578, Japan. Tel.: +81 22 795 5915; fax: +81 22 795 5504.
E-mail address: hirasawa@mail.pharm.tohoku.ac.jp (N. Hirasawa).

0923-1811/$36.00
doi:10.1016/j.jdermsci.2010.12.006

wire [14]. In this model, Ni wire but not Fe, Al and Co wires induced necrosis of the surrounding tissues. The implantation of the Ni wire elicited the increase in plasma exudation 8 h after the implantation and prostaglandin and histamine mediated the responses, indicating that Ni ions were released within a few hours [14].

LPS mimics the inflammation induced by an infection, which can occur when a biomedical device is implanted [15,16]. Therefore, it is possible that the injection of LPS enhances the elution of Ni ions from metals. In this study, using Ni wire-induced inflammation model and a novel *in vitro* system, we examined the mechanisms responsible for the elution of Ni.

2. Materials and methods

2.1. Animals

Male C57BL/6 mice, specific pathogen free and weighing 22–25 g, were purchased from SLC (Shizuoka, Japan). The mice were treated in accordance with procedures approved by the Animal Ethics Committee of Tohoku University, Japan.

2.2. Materials

A Ni wire (>99%, ϕ 0.8 mm), a SUS316L wire (ϕ 1 mm), and a Ni plate (>99%, thickness: 0.05 mm) were purchased from Nilako Co., Tokyo, Japan. Lipopolysaccharide (LPS) was purchased from Sigma–Aldrich (St. Louis, MO) and amiloride, chloroquine, and bafilomycin A_1 were from Wako Pure Chemical Ind. (Osaka, Japan).

2.3. Implantation of the Ni wire into mice

A nickel wire and a SUS316L wire were cut into 5 mm lengths and sterilized by soaking in ethanol. Mice were anesthetized and a length of wire was implanted subcutaneously in the dorsum using a 13G implant needle (Natsume Co., Tokyo, Japan). A hundred microliters of LPS solution (1 μg/ml) or saline was injected into the site immediately after the implantation. The mice were sacrificed at the indicated time and then the skin tissue (diameter: 14 mm) on the wire was excised. The skin samples were minced with scissors in 500 μl of Milli Q water and left at 4 °C overnight. The extract was centrifuged at 15,000 rpm for 20 min, and the supernatant was used to determine Ni concentrations as described below.

2.4. Determination of Ni concentrations by fluorometry and ICP-AES

Samples were diluted with Milli Q water, and Newport Green DCF [17] was added (150 μl per tube: 0.75 μM) to 850 μl of diluted sample. Fluorescence intensity was determined with excitation and emission wavelengths of 505 and 535 nm, respectively, with the use of a Fluorometer F-2000 (Hitachi High-Technologies Corporation, Japan). The Ni concentrations of some samples were determined by inductively coupled plasma atomic emission (ICP-AES) with an ICPS-8000 (Shimadzu System Development Corporation, Japan).

2.5. Macroscopic and histochemical analyses

Mice were sacrificed 0, 8, 24, or 72 h after the implantation. Tissue (14 mm in diameter) including epidermis, dermis and subcutaneous tissue on the wire was then excised and weighed. The wires obtained were washed with phosphate-buffered saline and then with an ice-cold lysis buffer (20 mM HEPES, pH 7.4, 1% (v/v) Triton-X 100, 10% (v/v) glycerol) to remove attached cells. The surface of wires was observed by scanning electric microscope (S-3200N, Hitachi, Japan).

2.6. Incubation of the Ni wire in vitro

A Ni wire was incubated in 50 μl of Milli Q water, saline, or mouse serum at 37 °C for 8 h. Then, the amount of Ni eluted was determined as described above.

2.7. Cell culture and stimulation

RAW 264 cells, mouse macrophage cell lines, were cultured at 37 °C under 5% CO_2–95% air in phenol red-free Eagle's minimal essential medium containing 10% (v/v) fetal bovine serum, penicillin G potassium (15 μg/ml), and streptomycin sulfate (50 μg/ml). The cells were suspended at the indicated numbers in the same medium, and 200 μl of the cell suspension was added to a Ni plate (25 mm^2) in each well of a 96-well cluster dish. Two hours later, LPS was added at the indicated concentrations and the cells were further incubated at 37 °C for 24 h or the period indicated. To prevent them attaching to plates, the cells were seeded first, and 2 h later, the Ni plate was placed in a sloping position into each well.

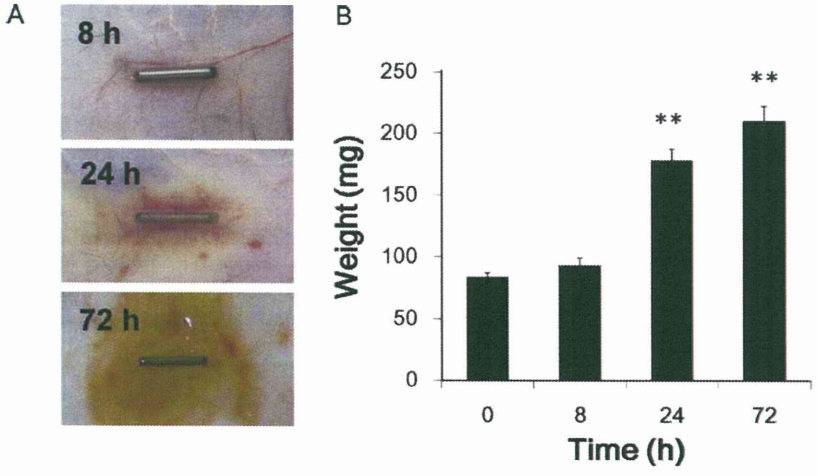

Fig. 1. Ni wire-induced inflammation. (A) A Ni wire was implanted subcutaneously in the dorsum of each mouse. The mice were sacrificed 8, 24 and 72 h after the implantation, and the skin around the wire was photographed. (B) The skin tissue (diameter: 14 mm) on the wire was excised and the weight of tissue was measured. The values are means for four mice with the S.E.M. shown by vertical bars. Statistical significance: $^{**}P < 0.01$ vs. the 0 h group.

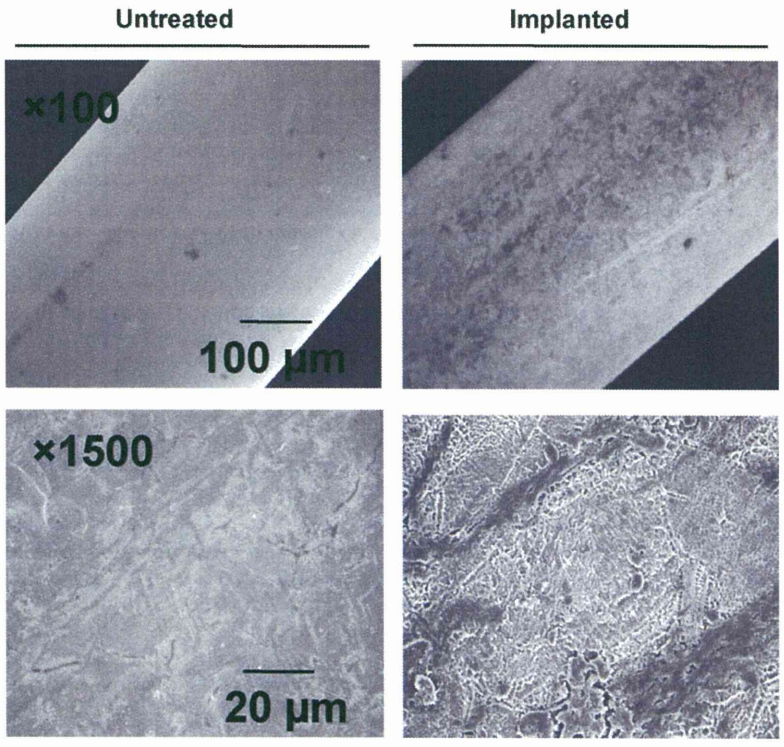

Fig. 2. Erosion of the surface of Ni wire. The surface of an untreated Ni wire (left) and an implanted Ni wire 72 h after implantation (right) was analyzed by scanning electron microscope.

2.8. Drug treatment

The V-ATPase inhibitor bafilomycin A_1 [18] was dissolved in DMSO, and the lysosome inhibitor chloroquine [19], and the Na^+/H^+ exchanger (NHE) inhibitor amiloride [20,21], were dissolved in autoclaved water, and diluted with the medium. The cells were incubated at 37 °C for 10 min in 1 ml of medium containing bafilomycin A_1 (1 nM), amiloride (100 μM), or chloroquine (10 μM) and then stimulated with LPS as described above. The final concentration of DMSO was 0.1% (v/v).

2.9. Statistical significance

The statistical significance of the results was analyzed with Dunnett's test or the Student–Newman–Keuls test for multiple comparisons. The results were confirmed by at least three independent sets of experiments.

3. Results

3.1. Metal wire-induced inflammation

A Ni wire was implanted subcutaneously into the dorsum of C57BL/6 mice and the response was observed 8, 24 and 72 h later. Consistent with our previous study, the wire caused extreme inflammation and bleeding (Fig. 1A). As an index of edema formation of tissues, the weight of skin tissues (14 mm in diameter) including epidermis, dermis and subcutaneous tissue on the wire was determined. The skin weight on the wire was

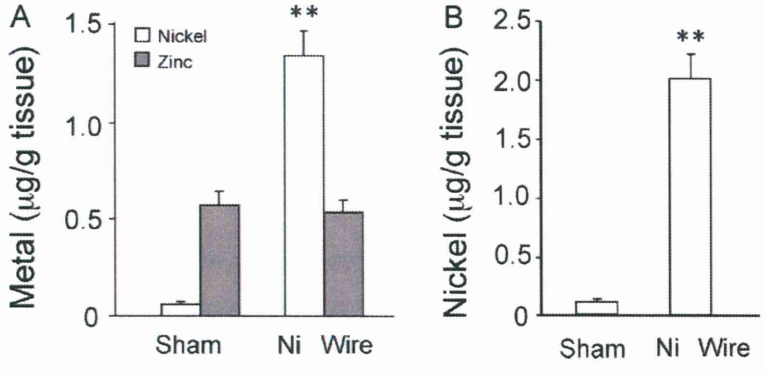

Fig. 3. Determination of the amount of Ni ions in tissues. (A) Skin tissue (diameter: 14 mm) was excised 8 h after the implantation of the Ni wire or sham treatment, and minced in 500 μl of deionized water. The concentrations of Ni and Zn ions in the supernatant were determined by ICP-AES. Values are the means for four mice with the S.E.M. shown by vertical bars. Statistical significance: $^{**}P < 0.01$ vs. the corresponding sham control group. (B) The concentrations of Ni in the same samples were determined by fluorometry. Values are means for four mice with the S.E.M. shown by vertical bars. Statistical significance: $^{**}P < 0.01$ vs. the sham group. The coefficient of the correlation between the concentrations of Ni ions determined by fluorometry (B) and by ICP-AES (A) was 0.996.

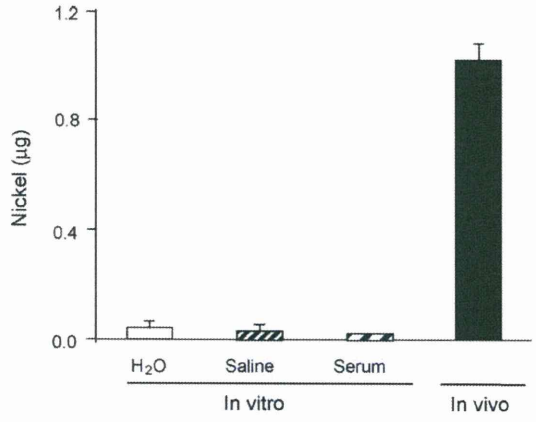

Fig. 4. Comparison of the release of Ni ions from a Ni wire *in vivo* and in solutions. A Ni wire was incubated at 37 °C for 8 h in 50 μl of H_2O, saline and serum. Then, Ni ions in the solution were quantified by fluorometry. The amount of Ni ions in the tissue 8 h after the implantation was determined as described in Fig. 3, and described as "*in vivo*". The values are the means of the four samples with S.E.M. shown by vertical bars.

significantly increased at 24 and 72 h (Fig. 1B), indicating that plasma leakage was induced by the Ni wire.

3.2. Corrosion of the wire

The corrosion of the implanted wire was analyzed with a scanning electron microscope. The untreated wire was smooth (Fig. 2, left panels) but the wire obtained 72 h after the implantation showed numerous traces of corrosion (Fig. 2, right panels), indicating that Ni ions had been released.

3.3. Quantitative analysis of the elution of Ni

A Ni wire was implanted subcutaneously in the dorsum and the skin tissue on the wire was excised 8 h later and homogenized. To evaluate quantitatively the release of Ni from the wire, the amounts of Ni ions, and Zn ions, as an internal control, in the supernatant of the skin tissue-homogenate were quantified by ICP-AES (Fig. 3A). The amount of Ni ions in the tissue was increased, although that of Zn ions was unchanged. Then we determined the concentration of Ni ions in the same sample by fluorometry using Newport Green DCF. As shown in Fig. 3B, the measurement of the Ni concentration in the control skin was not disturbed by Zn ions and the values showed a good correlation with those obtained by ICP-AES ($r = 0.996$). Therefore, in the experiment that followed, we determined the amount of Ni ions in the tissue by fluorometry.

3.4. Elusion of Ni ions in vivo and in solution

A Ni wire was incubated at 37 °C for 8 h in an aliquot of water, saline, or serum of C57BL/6 mice. The concentrations of Ni ions in the aliquots of water, saline and serum were only small as compared with the amount detected in the tissue homogenate (Fig. 4). These results suggested that Ni was eluted much more easily *in vivo* than *in vitro*.

3.5. Enhancement of the release of Ni from Ni- and SUS316L-wire in vivo by LPS

Using the wire-implanted mice, we found that the release of Ni ions was detectable at 8 h and increased to at least 72 h after the implantation. LPS (1 μg/100 μl saline) or saline (100 μl) was injected into the same site immediately after the implantation. Histological analysis disclosed that the wire's presence induced the infiltration of inflammatory cells, such as neutrophils and macrophages, in the tissue and LPS remarkably enhanced this process (Fig. 5A). The amount of Ni ions in the tissue samples from the LPS-treated group was significantly increased compared with that for the saline-treated group. The difference was significant at 8 and 24 h after the implantation (Fig. 5B).

Then we examined whether Ni was eluted from SUS316L, which is used as biomedical device. When SUS316L-wire was implanted subcutaneously in the dorsum of the mice, only a little elution of Ni ions was observed at 72 h after the implantation. As consistent with Ni wire, the elution of Ni from SUS316L wire was enhanced by the injection of LPS (Fig. 6).

3.6. Enhancement of the release of Ni ions from a metal plate by activated macrophages

Because macrophages are involved in the first line of defense in the inflammatory and immune response to foreign materials in

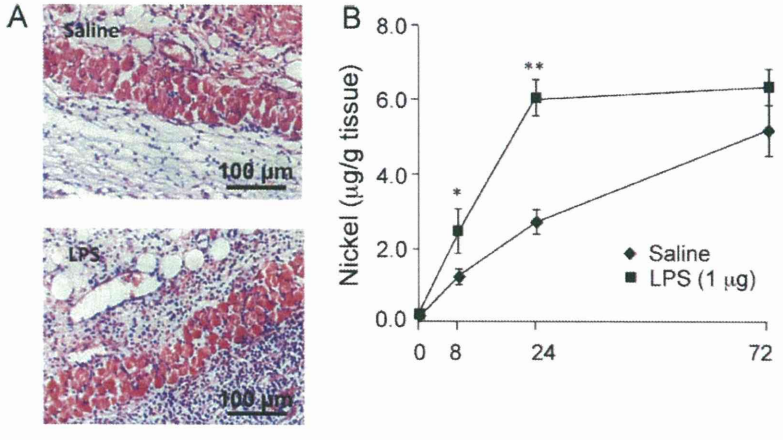

Fig. 5. Increase in the release of Ni ions by LPS-induced inflammation. (A) A Ni wire was implanted subcutaneously in the dorsum of each mouse. LPS (1 μg, bottom) or vehicle (saline, top) was injected into the site immediately after the implantation. Twenty-four hours after the implantation, the mice were sacrificed and the skin on the wire was dissected. Sections of tissue were prepared and stained with hematoxylin–eosin. (B) The skin tissue (diameter: 14 mm) on the wire was excised 8, 24 and 72 h after the implantation of Ni wires and the Ni ions in the tissue were quantified by fluorometry. Values are means for five mice with the S.E.M. shown by vertical bars. Statistical significance: $^*P < 0.05$, $^{**}P < 0.01$ vs. the saline group at the corresponding point.

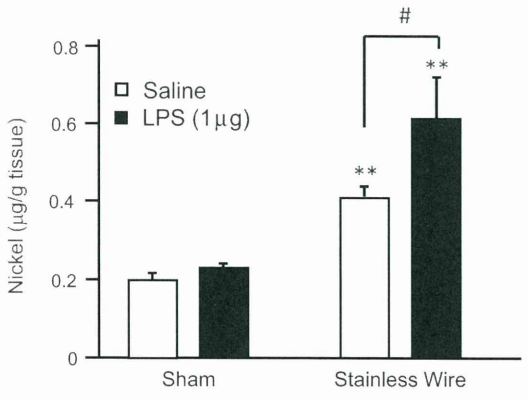

Fig. 6. Increase in the release of Ni ions from SUS316L by LPS. A SUS3167L-wire was implanted subcutaneously in the dorsum of each mouse. LPS (1 μg, closed columns) or vehicle (saline, open columns) was injected into the site immediately after the implantation. Seventy-two hours after the implantation, the mice were sacrificed and the skin tissue (diameter: 14 mm) on the wire was excised. The Ni ions in the tissue were quantified by fluorometry. Values are means for five mice with the S.E.M. shown by vertical bars. Statistical significance: $^{**}P < 0.01$ vs. the corresponding sham group, and $^{\#}P < 0.05$ between groups indicated.

many tissues, we examined whether these cells induced the release of Ni ions from metals by using a mouse macrophage cell line RAW 264. RAW 264 cells were seeded on a Ni plate (25 mm^2) and incubated for 24 h in the presence or absence of LPS (1 μg/ml). Although few Ni ions were released when the plate was incubated in medium alone, the amount increased in the presence of the cells (Fig. 7A). Interestingly, the stimulation of the cells with LPS significantly increased the release of Ni ions in a concentration- and time-dependent manner (Fig. 7B and C). These results suggested that the activated cells enhanced elution of Ni ions from the plate.

3.7. Change in pH of the conditioned medium

To clarify whether the elusion of Ni ions from plates was caused by acidification of the medium, the pH of the conditioned medium was determined. The pH of the conditioned medium collected after the 24-h incubation decreased dependent on the number of cells (Fig. 8A) but was not affected by the addition of LPS (Fig. 8B). These findings indicated that the acidification of the medium was induced by the respiratory metabolism of cells and was not the main cause to induce Ni elution.

3.8. Requirement of cell attachment to the metal

We examined whether the attachment of cells to the metal plate was required for LPS-induced enhancement of the release of Ni ions. The cells were incubated for 24 h either attached or unattached to the Ni plate, and the concentration of ions released was determined. In the absence of LPS, there was no difference in the release of Ni ions between the attached and unattached cultures (Fig. 9). However, LPS-induced enhancement of the elution was observed when the cells were attached

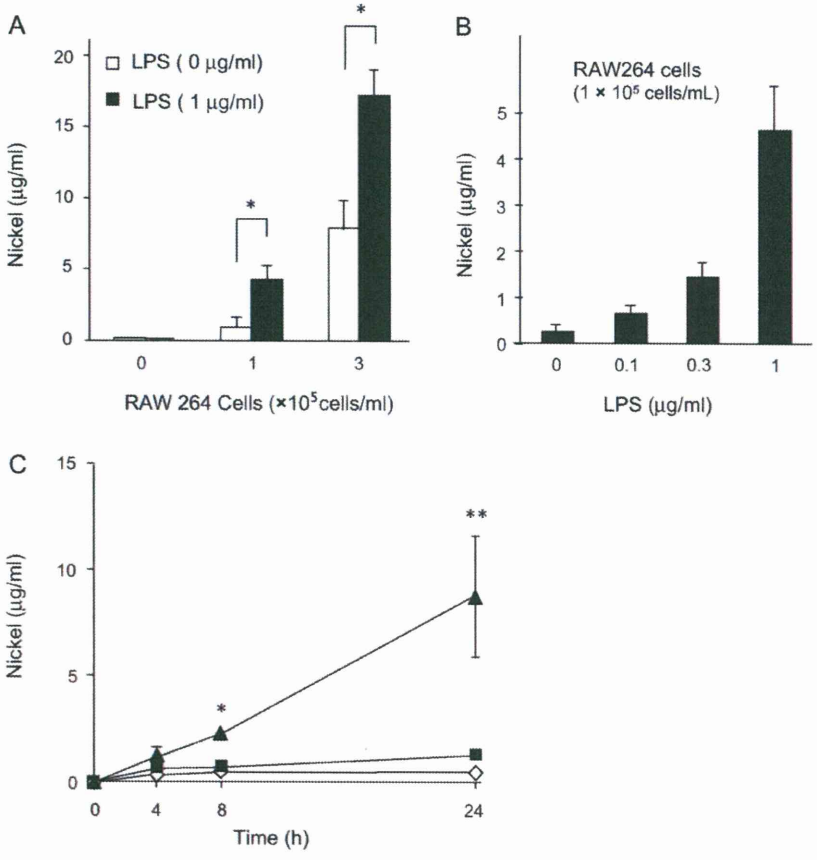

Fig. 7. Enhancement of elution of Ni ions from a Ni plate by LPS-stimulated RAW 264 cells. (A) The cells (1 or 3 × 10^5 cells/ml, 0.2 ml) seeded on a Ni plate (25 mm^2) were incubated for 24 h in the presence (closed columns) or absence (open columns) of LPS (1 μg/ml). The concentration of Ni ions in the supernatant was determined. (B) The cells (1 × 10^5 cells/ml, 0.2 ml) seeded on a Ni plate were incubated for 24 h in medium containing LPS (0.1, 0.3 and 1 μg/ml). (C) The cells (1 × 10^5 cells/ml, 0.2 ml) seeded on a Ni plate were incubated for 4, 8, and 24 h in medium containing LPS (1 μg/ml). Values are the means of five determinations with the S.E.M. shown by vertical bars. Statistical significance: $^{*}P < 0.05$, $^{**}P < 0.01$ vs. the corresponding LPS (0 μg/ml) group.

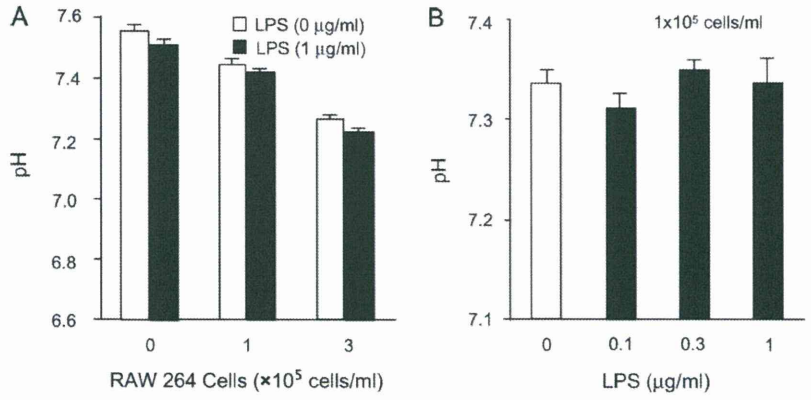

Fig. 8. Changes of pH in the culture medium of LPS-stimulated RAW 264 cells. The cells (1 and 3 × 10^5 cells/ml, 0.2 ml) seeded on a Ni plate (5 mm^2) were incubated for 24 h in the presence (closed columns) or absence (open columns) of LPS (1 μg/ml). The pH of the culture medium was determined with a pH meter. (B) The cells (1 × 10^5 cells/ml, 0.2 ml) seeded on a Ni plate (5 mm^2) were incubated for 24 h in medium containing LPS (0.1, 0.3 and 1 μg/ml). Values are the means for five determinations with the S.E.M. shown by vertical bars.

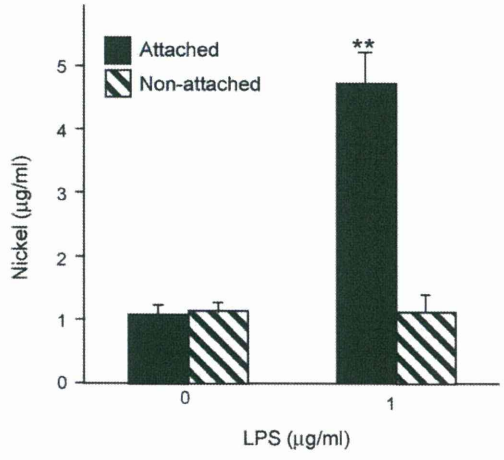

Fig. 9. Requirement of cell attachment for enhancement of the elution of Ni ions from Ni plates by LPS-stimulated RAW 264 cells. The cells (1 × 10^5 cells/ml, 0.2 ml) seeded on (attached condition) or under a Ni plate (non-attached condition) were incubated for 24 h in the presence or absence of LPS (1 μg/ml). The concentration of Ni in the culture medium was determined. Values are the means for five determinations with the S.E.M. shown by vertical bars. Statistical significance: $^{**}P < 0.01$ vs. the corresponding LPS (−) group.

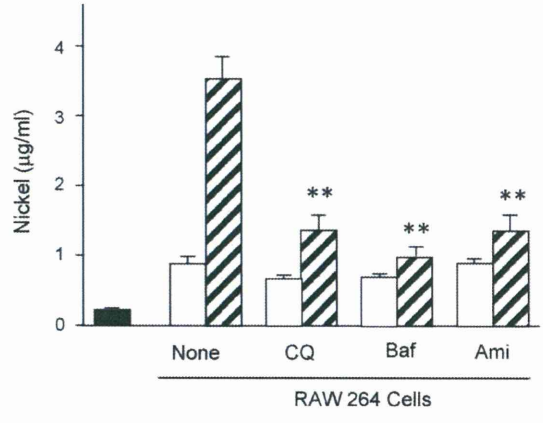

Fig. 10. Effects of inhibitors on the elution of Ni ions from Ni plates by RAW 264 cells. The cells (1 × 10^5 cells/ml, 0.2 ml) were seeded on a Ni plate (5 mm^2) and incubated for 24 h in medium containing chloroquine (CQ; 10 μM), amiloride (Ami; 100 μM) and bafilomycin A_1 (Baf; 1 nM) in the presence (hatched columns) and absence (open columns) of LPS (1 μg/ml). The closed column indicates that the Ni plate was incubated in the medium alone. The concentration of Ni in the supernatant was then determined. Values are the means for five determinations with the S.E.M. shown by vertical bars. Statistical significance: $^{**}P < 0.01$ vs. unstimulated RAW 264 cells, $^{\#\#}P < 0.01$ vs. LPS control.

to the plate (Fig. 9), indicating that the attachment of cells to plate was required to increase the release of Ni ions.

3.9. Effects of inhibitors on the release of Ni ions from the plates

The cells were incubated for 24 h on the Ni plate in the presence of the lysosome inhibitor chloroquine (10 μM), the V-ATPase inhibitor bafilomycin A_1 (1 nM), or the Na^+/H^+ exchanger (NHE) inhibitor amiloride (100 μM), and the concentration of Ni ions in the medium was determined. These inhibitors failed to reduce the release of Ni ions in the absence of LPS, but apparently inhibited it in the presence of LPS (Fig. 10). In the absence of the Ni plate, these inhibitors did not affect the viability of the cells (data not shown). These findings suggested that the release of H^+ by the cells was induced by the stimulation with LPS and caused the release of Ni ions from the plate.

4. Discussion

In this study, using two newly established models to assess the corrosion of Ni *in vivo* and *in vitro*, we found that inflammatory cells accelerated the release of Ni ions from the surface of the metal.

We developed a fluorometric method to determine Ni concentrations in tissue homogenate using Newport Green DCF, an indicator of Zn and Ni ions [17]. The Ni content obtained by the fluorometric assay well correlated with that obtained by ICP-AES, indicating the physiological concentration of Zn ions to be negligible in the fluorometric assay. In this study, we employed wires and plates made of >99% Ni to maximize the release of Ni from alloys. Therefore, the fluorometric assay was a convenient way to determine the concentration of Ni ions. For biomedical alloys such as stainless steel and nitinol, ICP-AES or ICP-MS should be used to assess the release of several metal ions at the same time. Such models are now under investigation.

Interestingly, when the wire was incubated at 37 °C for 8 h in water, saline, or mouse serum, only a little Ni was released. However, Ni ions were released more easily when the wire was implanted subcutaneously in mice, indicating the release to be highly dependent on the activation of cells around the wire. The increase in the concentration of Ni ions around the wire was already evident at 8 h after the implantation and well-correlated with the increase in vascular permeability [14]. Wataha et al. determined the concentration of Ni using a laser-ablation technique in tissue collected 7 days after implantation and demonstrated that the

distribution of the ions correlated well with the extent of necrosis in a Ni wire-implantation model in rats [22]. Therefore, it was likely that the eluted Ni ions caused local inflammation. The finding that the release of Ni ions into tissue was significantly increased by the injection of LPS suggested that the activation of inflammatory cells was involved in the corrosion of the wire. This notion was confirmed *in vitro* using RAW 264 cells. Namely, although little Ni was released from the plate in the medium alone, a significant increase in the elution was elicited in the presence of the cells, and apparently enhanced by the addition of LPS.

This *in vitro* model was useful for clarifying the molecular mechanisms by which activated inflammatory cells elute metals. LPS and inflammatory cytokines such as IL-1 activated V-ATPase and NHE in macrophages [23,24]. The unstimulated cells released a few Ni ions in both attached and unattached cultures and the release was little affected by the three inhibitors. The LPS-enhanced elution of Ni ions was observed only when the cells were attached to the metal and was markedly inhibited by chloroquine, bafilomycin A_1 and amiloride. Similar findings were observed regarding the resorption of bone by osteoclasts [25–27]. Osteoclasts attach to the bone and form a specialized compartment, the sealing zone, in which the resorption of bone is induced. Osteoclasts acidify the space using V-ATPase [28,29]. Because chloroquine neutralizes the acidity and the inhibitor of V-ATPase blocked the acidification, both inhibitors potently suppress bone resorption [30,31]. In addition, the NHE inhibitor also inhibited bone resorption and acidification [32], although the molecular mechanisms involved are not completely clear. However, amiloride inhibits the LPS-induced activation of cells [33,34]. Taken together, the molecular mechanisms of the elution of Ni might be similar to those behind the resorption of bone by osteoclasts. Recently, it was reported that macrophages create the acidic extracellular compartment to aggregated lipoproteins, which was inhibited by bafilomycin A_1 [35]. Thus, macrophages also form the acidic compartment via V-ATPase in various inflammatory processes. These findings suggest that the LPS-stimulated cells on Ni plates form a compartment and acidify it via V-ATPase and NHE, resulting in the elution of Ni ions.

Metal allergy is a concern when using metallic biomedical devices. Since we usually intake Ni ions from foods, the increase in the concentration of Ni ions in plasma might not be enough to induce Ni-allergy. There is a possibility that additional factor such as the exposure to LPS was required to elicit the sensitization of Ni [10]. On the other hand, in the Ni-sensitized persons, the elution of Ni ions from biomedical devices causes Ni-allergy. The most effective way to avoid it is to block the release of metal ions from biomaterials. However, there has been no system to assess the corrosion of metals under inflammatory conditions. We established *in vivo* and *in vitro* models for assessing the release of Ni from metal. In these models, the activation of cells such as macrophages apparently enhanced the corrosion of Ni. Thus, to assess the safety of biomaterials, the release of metal ions under inflammatory conditions should be evaluated. Our models might be useful tools for this purpose. Notably, the *in vitro* model might reflect the elution of Ni at sites of inflammation *in vivo*.

In conclusion, the elution of Ni ions from metal devices was promoted by inflammatory cells attached to the surface and inflammation as well as infection might augment the elution by enhancing the efflux of proton into the sealing zone as is the case for bone resorption.

Acknowledgements

This study was partly supported by Grants-in Aid for Science Research from the Ministry of Health, Labour, and Welfare of Japan, and the Cosmetology Research Foundation.

References

[1] Lee K, Goodman SB. Current state and future of joint replacements in the hip and knee. Expert Rev Med Devices 2008;5:383–93.
[2] Gotman I. Characteristics of metals used in implants. J Endocrinol 1997;11:383–9.
[3] Niinomi M. Metallic biomaterials. J Artif Organs 2008;11:105–10.
[4] Basketter DA, Briatico-Vangosa G, Kaestner W, Lally C, Bontinck WJ. Nickel, cobalt and chromium in consumer products: a role in allergic contact dermatitis? Contact Dermatitis 1993;28:15–25.
[5] Hostynek JJ. Nickel-induced hypersensitivity: etiology, immune reactions, prevention and therapy. Arch Dermatol Res 2002;294:249–67.
[6] Van den Broeke LT, Heffler LC, Linder T, Nilsson JLG, Karlberg AT, Scheynius S. Direct Ni^{2+} antigen formation on cultured human dendritic cells. Immunology 1999;96:578–85.
[7] Thierse HJ, Gamerdinger K, Junkes C, Guerreiro N, Weltzien HU. T cell receptor (TCR) interaction with haptens: metal ions as non-classical haptens. Toxicology 2005;209:101–7.
[8] Artik S, von Vultée C, Gleichmann E, Schwarz T, Griem P. Nickel allergy in mice: enhanced sensitization capacity of nickel at higher oxidation states. J Immunol 1999;163:1143–52.
[9] Artik S, Haarhuis K, Wu X, Begerow J, Gleichmann E. Tolerance to nickel: oral nickel administration induces a high frequency of anergic T cells with persistent suppressor activity. J Immunol 2001;167:6794–803.
[10] Sato N, Kinbara M, Kuroishi T, Kimura K, Iwakura Y, Ohtsu H, et al. Lipopolysaccharide promotes and augments metal allergies in mice, dependent on innate immunity and histidine decarboxylase. Clin Exp Allergy 2007;37:743–51.
[11] Ishii N, Moriguchi N, Nakajima H, Tanaka S, Amemiya F. Nickel sulfate-specific suppressor T cells induced by nickel sulfate in drinking water. J Dermatol Sci 1993;6:159–64.
[12] Ishii N, Sugita Y, Nakajima H, Tanaka S, Askenase PW. Elicitation of nickel sulfate ($NiSO_4$)-specific delayed-type hypersensitivity requires early-occurring and early-acting, $NiSO_4$-specific DTH-initiating cells with an unusual mixed phenotype for an antigen-specific cell. Cell Immunol 1995;161:244–55.
[13] Takeuchi O, Akira S. Toll-like receptors; their physiological role and signal transduction system. Int Immunopharmacol 2001;1:625–35.
[14] Hirasawa N, Goi Y, Tanaka R, Ishihara K, Ohtsu H, Ohuchi K. Involvement of prostaglandins and histamine in nickel wire-induced acute inflammation in mice. J Biomed Mater Res 2010;93A:1306–11.
[15] Zimmerli W. Infection and musculoskeletal conditions: prosthetic-joint-associated infections. Best Pract Res Clin Rheumatol 2006;20:1045–63.
[16] Ochoa RA, Mow CS. Deep infection of a total knee implant as a complication of disseminated pneumococcal sepsis. A case report and review of literature. Knee 2008;15:144–7.
[17] Thierse HJ, Helm S, Pink M, Weltzien H. Novel fluorescence assay for tracking molecular and cellular allergen–protein interactions. J Immunol Methods 2007;328:14–20.
[18] Bowman EJ, Siebers A, Altendorf K. Bafilomycins: a class of inhibitors of membrane ATPase from microorganisms, animal cells, and plant cells. Proc Natl Acad Sci USA 1988;85:7972–6.
[19] De Duve C, De Barsy T, Poole B, Trouet A, Tulkens P, Van Hoof F. Lysosomotropic agents. Biochem Pharmacol 1974;24:2495–531.
[20] Kleyman TR, Cragoe Jr EJ. Amiloride and its analogs as tools in the study of ion transport. J Membr Biol 1988;105:1–21.
[21] Masereel B, Pochet L, Laeckmann D. An overview of inhibitors of Na^+/H^+ exchanger. Eur J Med Chem 2003;38:547–54.
[22] Wataha JC, O'Dell NL, Singh BB, Ghazi M, Whitford GM, Lockwood PE. Relating nickel-induced tissue inflammation to nickel release in vivo. J Biomed Mater Res 2001;58:537–44.
[23] Brisseau GF, Grinstein S, Hackam DJ, Nordström T, Manolson MF, Khine AA, et al. Interleukin-1 increases vacuolar-type H+-ATPase activity in murine peritoneal macrophages. J Biol Chem 1996;271:2005–11.
[24] Vairo G, Royston AK, Hamilton JA. Biochemical events accompanying macrophage activation and the inhibition of colony-stimulating factor-1-induced macrophage proliferation by tumor necrosis factor-α, interferon-γ and lipopolysaccharide. J Cell Physiol 1992;151:630–41.
[25] Shibata T, Amano H, Yamada S, Ohya K. Mechanisms of proton transport in isolated rat osteoclasts attached to bone. J Med Dent Sci 2000;47:177–85.
[26] Evans RW, Cheung HS, McCarty DJ. Cultured human monocytes and fibroblasts solubilize calcium phosphate crystals. Calcif Tissue Int 1984;36:645–50.
[27] Blair HC, Athanasou NA. Recent advances in osteoclast biology and pathological bone resorption. Histol Histopathol 2004;19:189–99.
[28] Henriksen K, Sorensen MG, Jensen VK, Dziegiel MH, Nosjean O, Karsdal MA. Ion transporters involved in acidification of the resorption lacuna in osteoclasts. Calcif Tissue Int 2008;83:230–42.
[29] Xu J, Cheng T, Feng HT, Pavlos NJ, Zheng MH. Structure and function of V-ATPases in osteoclasts: potential therapeutic targets for the treatment of osteolysis. Histol Histopathol 2007;22:443–54.
[30] Kwong CH, Burns WB, Cheung HS. Solubilization of hydroxyapatite crystals by murine bone cells, macrophages and fibroblasts. Biomaterials 1989;10:579–84.
[31] Yao G, Feng H, Cai Y, Qi W, Kong K. Characterization of vacuolar-ATPase and selective inhibition of vacuolar-H(+)-ATPase in osteoclasts. Biochem Biophys Res Commun 2007;357:821–7.

[32] Heming TA, Bidani A. Intracellular pH regulation in U937 human monocytes: roles of V-ATPase and Na^+/H^+ exchange. Immunobiology 2003;207:141–8.
[33] Haddad JJ, Land SC. Amiloride blockades lipopolysaccharide-induced proinflammatory cytokine biosynthesis in an IkB-a/NF-kB-dependent mechanism. Evidence for the amplification of an antiinflammatory pathway in the alveolar epithelium. Am J Respir Cell Mol Biol 2002;26:114–26.
[34] Kamachi F, Ban HS, Hirasawa N, Ohuchi K. Inhibition of lipopolysaccharide-induced prostaglandin E_2 production and inflammation by the Na^+/H^+ exchanger inhibitors. J Pharmacol Exp Ther 2007;321:345–52.
[35] Haka AS, Grosheva I, Chiang E, Buxbaum AR, Baird BA, Pierini LM, et al. Macroophages create an acidic extracellular hydrolytic compartment to digest aggregated lipoproteins. Mol Biol Cell 2009;20:4932–40.

Mini Review

Assessment of the release of nickel from biomaterials in vivo and in vitro: enhancement by lipopolysaccharide

Rina Tanaka[1)], Yoshiaki Goi[1)], Kenji Ishihara[2)], Kyosuke Ueda[3)], Takayuki Narushima[3)], Hiroshi Ohtsu[3)], Kazuo Ohuchi[4)], Masahiro Hiratsuka[1)] and Noriyasu Hirasawa[1, *)]

[1)]Graduate School of Pharmaceutical Sciences, Tohoku University, Japan
[2)]Course for School Nurse Teacher, Faculty of Education, Ibaraki University, Japan
[3)]Graduate School of Engineering, Tohoku University, Japan
[4)]Faculty of Pharmacy, Yasuda Women's University, Japan

Biodevices are implanted for long periods of time, so the release of metal ions from alloys should be tested in tissues to assess the risk of inducing metal allergies. However there is little evidence that the release of metal ions from alloys *in vivo* is similar to that *in vitro*. We implanted metal wires in mice and determined the concentration of metal ions in tissue to analyze the mechanisms responsible for metal allergies. The release of ions from the Ni wire was detected within 8 h and attained a plateau 72 h after the implantation. Furthermore, it was significantly increased by an injection of LPS. The results indicated that the release of Ni was apparently enhanced by inflammatory responses. We also established an *in vitro* assay system using the murine macrophage cell line RAW 264. The addition of LPS apparently increased the amount of Ni released into the medium, indicating the activation of the cells to have enhanced the elution of ions from the Ni plate. Our *in vitro* model using LPS-stimulated RAW264 cells might reflect the elution of Ni in inflamed tissue.

Rec.4/5/2010, Acc.11/9/2010

*Correspondence should be addressed to:
Noriyasu Hirasawa, Ph.D., Laboratory of Pharmacotherapy of Life-style Related Diseases, Graduate School of Pharmaceutical Sciences, Tohoku University, Sendai, Miyagi 980-8578, Japan. Phone: +81-22-795-5915, Fax: +81-22-795-5504, e-mail: hirasawa@mail.pharm.tohoku.ac.jp

Key words:
Nickel release, lipopolysaccharide, in vivo model, in vitro model, RAW264 cells

Introduction

Implantations of biomedical devices to treat diseases and organ insufficiencies are increasing as populationage [1]. Most devices for the replacement of hard tissues, including artificial hip joints, bone plates and dental implants, comprise metallic biomaterials because of their reliable mechanical performance [2-3]. Corrosion-resistant and ductile[3] nickel (Ni) is contained in various alloys, including stainless steels, Ni-Cr and Ni-Ti. However, Ni is also the most common contact allergen among metals[4-5]. Allergies to Ni, classified as Type IV allergies [4-6], are initiated by the release of Ni ions from alloys and the forming of Ni-binding proteins, which are recognized as antigens by antigen-presenting cells such as dendritic cells (DC) and macrophages [4]. These cells then activate T cells and induce an increase in the number of Ni-specific, IFN-γ-producing $CD4^+$ and $CD8^+$ effector T cells[4-6]. It is difficult to prevent Ni allergies by inhibiting these immune responses. A more practical approach might be to block the elution of Ni ions from biomaterials. However, the molecular mechanisms of this elution have not been fully examined.

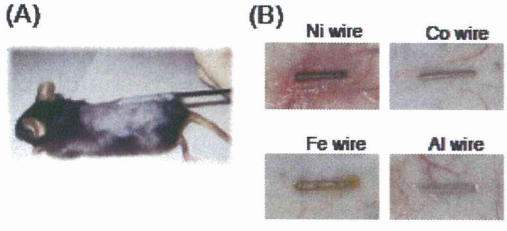

Fig. 1. Metal wire-implanted mice
A metal wire was implanted subcutaneously in the dorsum with an implant needle (A). The mice were sacrificed 72 h after the implantation and the skin around the wire was photographed (B, modified from ref. 17).

In general, the release of Ni ions from alloys is tested in solutions. For example, Okazaki *et al.* determined the release of metal ions from SUS316L stainless steel and Co–Cr–Mo casting alloy immersed in α-medium, PBS (−), calf serum, 0.9% NaCl, artificial saliva, 1.2 % L-cysteine, 1 % lactic acid and 0.01 % HCl for 7 days [7]. As biodevices are implanted for long periods of time, one should test the release of metal ions from alloys in tissues to assess the risk of inducing metal allergies. However, there is little evidence that the release of metal ions from alloys *in vivo* is similar to that *in vitro*.

Animal models of Ni-induced allergy and inflammation

To reveal the mechanisms of Ni-induced inflammation and allergy, several animal models have been developed. The injection of Ni ions into sensitized animals was found to cause allergic inflammation including ear swelling[8-10], footpad edema[12] and the proliferation of lymph node cells[8, 12]. Tolerance to nickel sensitization was also examined in these models[9, 11]. However, it is much more difficult to induce an allergy to Ni than to a proteinous antigen. In general, a high concentration of Ni or an oxidized form of the ion such as Ni (III) or Ni (IV) is required to trigger inflammation or an allergy[8]. Recently, Sato et al. found that the co-administration of lipopolysaccharide (LPS), a stimulator of innate immune responses, effectively enhanced sensitization to Ni [10]. Sensitization using Ni ions plus LPS will promote research into the evocation of Ni allergies. In addition, the toxicity of Ni particles to lung was assessed by injecting intratracheally in rats and mice[13-15]. The Ni particles induced the infiltration of leukocytes in bronchalveolar lavage fluid and production of tumor necrosis factor-α in this model[15]. Wataha *et al.* implanted a Ni wire into the subcutaneous space of rats and analyzed Ni concentrations in tissues and necrosis[16]. According to the methods described by Wataha et al., we implanted a metal subcutaneously in the dorsum of mice using an implant needle (Fig. 1A). We examined the effects of Ni and Co wires because Ni and Co were well-known metals inducing metal allergy. In addition, the Fe and Al wires were used as the control to clarify the nonspecific inflammation induced by the implantation of wires. The Ni wire caused extreme inflammation but the Co, Fe, and Al wires did not (Fig. 1B), indicating that Ni ions are easily released and cause inflammation[17]. In this model, the Ni wire-induced inflammation was assessed as the increase in vascular permeability, which was determined by the leakage of Evans blue[17]. The implantation of Ni wire also induced the expression of cyclooxygease-2 and histidine decarboxylase in the surrounding tissues[17].

Quantitative analysis of ions release from the implanted Ni wire

Analytical techniques like inductively coupled plasma-atomic emission spectrometry (ICP-AES) and ICP-Mass spectrometry (MS) are used for the detection of metals in solution. Wataha *et al.* analyzed Ni concentrations in tissues around the Ni wire 48 h, 96 h and 7 days later using laser-ablation (LA)-ICP-MS [16]. They found that the Ni caused severe inflammation and necrosis, and that its distribution in tissues correlated well with the inflammation. They appeared that greater than 25 μg/g of Ni in tissue was necessary to elicit severe inflammation with necrosis. In *in vitro* experiments using fibroblasts, endothelial cells, and monocytes, 10-50 μg/ml of Ni ions cause total suppression of mitochondrial function [18-20]. However, the concentration at which Ni ions induce Ni allergy has not been determined. Therefore, the quantitative analysis of the release of Ni ions from materials *in vivo* is required to assess the safety of biomaterials. We developed a fluorometric assay to determine Ni concentrations using Newport Green. Thierse et al. examined the binding of Ni to membranes of human Raji B cells by flow cytometry with Newport Green [21]. The use of Newport Green will reveal where Ni binds to protein as well as its concentration in tissues. Using the Ni wire-implanted mice described above, we determined the concentration of Ni in tissue and found that the release of Ni ions was detectable within 8 h and attained a plateau 72 h after the implantation. Vascular permeability around the wire also increased from 8 h post-implantation [16]. Interestingly, when the wire was incubated at 37 °C for 8 h in water, saline, or mouse serum, very little Ni was released. Thus, Ni ions were released more easily *in vivo* than in the solutions, indicating the release to be highly dependent on the responses of cells around the wire.

Enhancement by lipopolysaccharide of the release of Ni ions *in vivo*

The implantation of biomedical devices can cause infections and bacteria-induced inflammation. Although the inflamed sites become acidic, it is not clear whether the infection and inflammation affect the elution of Ni. So we examined the involvement of inflammatory responses in the release of Ni *in vivo*. LPS (1 μg/ 200 μL saline) was injected subcutaneously around the wire at the time of implantation. The release of Ni ions into tissue was significantly increased by the injection of LPS compared to an injection of the vehicle only. These results clearly indicated that the release of Ni was enhanced by the inflammatory responses. Thus, the elution of metal ions was induced by the attached cells on the surface of alloys and enhanced by inflammatory stimuli. These findings suggested that the release of metal ions from biomaterials in buffers might not reflect that in tissues. Thus, our metal-wire implant model might be used to assess the safety of biomaterials in normal tissues and in the inflammatory conditions.

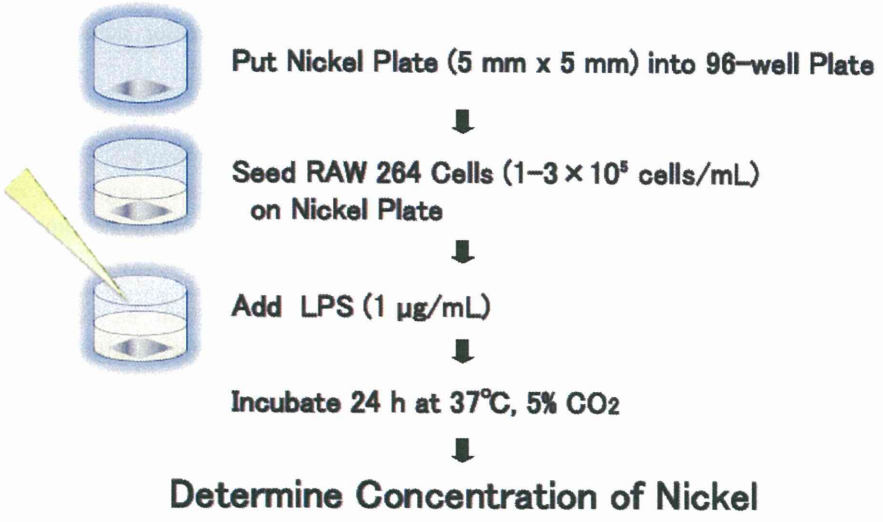

Fig. 2. ***In vitro*** **assay system for Ni release from the plate**

In vitro system for the assessment of Ni release at inflamed sites

The effects of inflammatory responses to infections on the release of Ni from alloys have not been analyzed *in vitro*. The finding that LPS enhanced the release of ions from a Ni wire implanted in mice, however, indicates that the corrosion of metals should be tested under condition similar to those in inflamed tissue. Consequently, we established an *in vitro* assay system using the murine macrophage cell line RAW 264 as the inflammatory cells activated by LPS (Fig. 2). RAW 264 cells were seeded on a Ni plate (5 mm square) and incubated for 4, 8 and 24 h in the presence or absence of LPS. Although little Ni was released from the plate in the medium alone, a significant increase occurred in the presence of the cells. LPS (0.1 to 1 μg/mL) significantly enhanced the release of Ni into the medium in concentration- and time-dependent manners, indicating that the activation of RAW 264 cells enhanced the elution of ions from the plate. These findings suggested our *in vitro* model using LPS-stimulated RAW264 cells to be a novel system reflecting the elution of Ni at the site of inflammation.

Our findings indicated that the interaction of the cells with metals on its surface is important to release of metal ions. However, it has not been disclosed that the molecular mechanisms by which activated inflammatory cells elute metal ions from the surface of metals. Our *in vitro* model using macrophages is useful to analyze the mechanisms.

Conclusion

Metal allergy is a concern when using biomedical devices containing metals. The most effective way to avoid it is to block the release of metal ions from biomaterials. However, assay systems had not been able to assess the corrosion of metals under inflammatory conditions. We established *in vivo* and *in vitro* models for assessing the release of Ni from metal. In these models, the activation of cells such as macrophages apparently enhanced the corrosion of Ni. Thus, to assess the safety of biomaterials, one should evaluate the release of metal ions under inflammatory conditions. Our models might be useful tools for this purpose. We employed Ni wires and plates to maximize the release of Ni. If using ICP-APS and ICP-MS within our models, the release of various metal ions from biomedical alloys could be assessed at the same time.

References

1) Lee K, Goodman SB: Current state and future of joint replacements in the hip and knee. Expert Rev Med Devices. 2008; 5: 383-393.

2) Gotman I: Characteristics of metals used in implants. J Endocrinol. 1997; 11: 383-389.

3) Niinomi M: Metallic biomaterials. J Artif Organs. 2008; 11: 105-110.

4) Basketter DA, Briatico-Vangosa G, Kaestner W, Lally C, Bontinck WJ: Nickel, cobalt and chromium in consumer products: a role in allergic contact dermatitis? Contact Dermatitis. 1993; 28: 15-25.

5) Czarnobilska E, Obtułowicz K, Wsołek K, Pietowska J, Spiewak R: Mechanisms of nickel allergy. Przegl Lek. 2007; 64: 502-505.

6) Thierse HJ, Gamerdinger K, Junkes C, Guerreiro N, Weltzien HU: T cell receptor (TCR) interaction with haptens: metal ions as non-classical haptens. Toxicology. 2005; 209: 101-107.

7) Okazaki Y, Gotoh E: Comparison of metal release from various metallic biomaterials in vitro. Biomaterials. 2005; 26: 11-21.

8) Artik S, von Vultée C, Gleichmann E, Schwarz T, Griem P: Nickel allergy in mice: enhanced sensitization capacity of nickel at higher oxidation states. J Immunol. 1999; 163: 1143-1152.

9) Artik S, Haarhuis K, Wu X, Begerow J, Gleichmann E: Tolerance to nickel: oral nickel administration induces a high frequency of anergic T cells with persistent suppressor activity. J Immunol. 2001; 167: 6794-6803.

10) Sato N, Kinbara M, Kuroishi T, Kimura K, Iwakura Y, Ohtsu H, Sugawara S, Endo Y: Lipopolysaccharide promotes and augments metal allergies in mice,dependent on innate immunity and histidine decarboxylase. Clin Exp Allergy 2007; 37: 743-751.

11) Ishii N, Moriguchi N, Nakajima H, Tanaka S, Amemiya F: Nickel sulfate-specific suppressor T cells induced by nickel sulfate in drinking water. J Dermatol Sci.1993; 6: 159-164.

12) Ishii N, Sugita Y, Nakajima H, Tanaka S, Askenase PW: Elicitation of nickel sulfate (NiSO4)-specific delayed-type hypersensitivity requires early-occurring and early-acting, NiSO4-specific DTH-initiating cells with an unusual mixed pheno-

type for an antigen-specific cell. Cell Immunol. 1995; 161: 244-255.

13) Benson, JM, Burt, RL, Carpenter, RL, Edison, AF, Hahn, FF, Haley, PJ, Hanson, PJ, Hanson, RL, Hobbs, CH, Pickrell, JA, Dunnick, JK: Comarative inhalation toxicity of nickel sulfate to F344/N rats and B6C3F1 mice exposed for 12 days. Fundam Appl Toxicol. 1988; 9: 252-265.

14) Benson JM, Burt, RL, Cheng YS, Hahn, FF, Haley, PJ, Henderson, RF, Hobbs, CH, Pickrell, JA, Dunnick, JK: Biochemical responses of rats and mouse lung to inhaled nickel compounds. Toxicol. 1989; 57: 255-266.

15) Zhang, Q, Kusama, Y, Zhu, X, Sato, K, Mo, Y, Kluz, T, Donaldson, K: Comparative toxicity of standard nickel and ultrafine nickel in lung after intratracheal instillation. J. Occup Health. 2003; 45: 23-30.

16) Wataha JC, O'Dell NL, Singh BB, Ghazi M, Whitford GM, Lockwood PE: Relating nickel-induced tissue inflammation to nickel release in vivo. J Biomed Mater Res. 2001; 58: 537-544.

17) Hirasawa N, Goi Y, Tanaka R, Ishihara K, Ohtsu H, Ohuchi K: Involvement of prostaglandins and histamine in nickel wire-induced acute inflammation in mice. J Biomed Mater Res A. 2010; 93: 1306-1311.

18) Wataha JC, Hanks CT, Craig RG: The in vitro effects of metal cations on eulariotic cell metabolism. J Biomed Mater Res. 1991; 25: 1133-1149.

19) Wataha JC, Hanks CT, Sun ZL: In vitro reaction of macrophages to metal ions from dental biomaterials. Dent Mater. 1995; 11: 239-245.

20) Wataha JC, Sun ZL, Hanks CT, Fang DN: Effects of Ni ions on expression of intercellular adhesion molecule 1 by endothelial cells. J Biomed Mater Res. 1997; 36: 145-151.

21) Thierse HJ, Helm S, Pink M, Weltzien H: Novel fluorescence assay for tracking molecular and cellular allergen-protein interactions. J Immunol Methods. 2007; 328: 14-20.